Protein Recognition Motifs: Design of Peptidomimetics of Helix Surfaces

Ye Che,[1] Bernard R. Brooks,[1] Garland R. Marshall[2]

[1] *Laboratory of Computational Biology, National Heart, Lung and Blood Institute, National Institutes of Health, Bethesda, MD 20892*

[2] *Center for Computational Biology and Department of Biochemistry and Molecular Biophysics, WA University, St. Louis, MO 63110*

Received 30 December 2006; revised 29 March 2007; accepted 9 April 2007
Published online 18 April 2007 in Wiley InterScience (www.interscience.wiley.com). DOI 10.1002/bip.20744

ABSTRACT:

Helices represent one of the most common recognition motifs in proteins. The design of nonpeptidic scaffolds, such as the 3,2′,2″-tris-substituted terphenyl, that can imitate the side-chain orientation along one face of an α-helix potentially provides an effective means to modulate helix-recognition functions. Here, based on theoretical arguments, we described novel α-helix mimetics which are more effective than the terphenyl at constraining the aryl–aryl torsion angles to those associated with structures suitable for mimicking the α-helical twist for side-chain orientation and for superimposing the side chains of residues i, i + 3 *or* i + 4, i + 7 *when compared with the α–β side-chain vectors of the regular α-helix with an improved root mean square deviation (RMSD) of approximately 0.5 Å. In addition, this study suggests that rotamer distributions around the* C_α—C_β *bonds of these helix mimetics are similar to those of α-helices, except that these rotamer distributions show an approximately 60° shift compared to those of α-helices when the mimetic axis is superimposed upon the helix axis. This change in rotamer orientation complicates mimicry of the helix surface.* © *2007 Wiley Periodicals, Inc.*† *Biopolymers 86: 288–297, 2007.*

Keywords: α-helix; peptidomimetic; template design; privileged structure; conformational analysis; side-chain

This article was originally published online as an accepted preprint. The "Published Online" date corresponds to the preprint version. You can request a copy of the preprint by emailing the Biopolymers editorial office at biopolymers@wiley.com

Correspondence to: Ye Che; e-mail: chey@nhlbi.nih.gov
Contract grant sponsor: Intramural Research Program of the NIH, NHLBI
Contract grant sponsors: NIH
Contract grant number: GM 68460
This article contains supplementary material available via the Internet at http://www.interscience.wiley.com/jpages/0006-3525/suppmat

INTRODUCTION

α-Helices on protein surfaces often function as recognition motifs for protein–protein, protein–DNA, and protein–RNA interactions. Consequently, these helical recognition motifs represent attractive targets for potential therapeutics in a broad spectrum of diseases.[1] Typically, however, short peptides corresponding to such helical motifs do not fold stably in isolation and are usually flexible and conformationally disordered in solution. Such flexible peptides present side chains in a plethora of relative orientations increasing undesirable interactions at multiple recognition sites. This inherent flexibility also limits binding affinity when these peptides bind to their targeted receptors in a unique conformation due to a more significant loss of entropy. It is estimated (see Mam-

mon et al.[2] for a thorough discussion of torsional entropy) that elimination of a single rotational degree of freedom of a peptide by preorganization to stabilize the receptor-bound conformation enhances affinity by approximately 1.2–1.6 kcal/mol assuming complete loss of rotational degrees of freedom.[3,4] Thus, preorganization of even a 10-residue helical segment with multiple (18–20) rotational degrees of freedom in the peptide backbone, for example, into its receptor-bound conformation should enhance the binding affinity by orders of magnitude.

Accordingly, numerous strategies have been developed to stabilize helical conformations of a peptide.[5] Marshall and Bosshard[6] predicted in 1972 that α,α-dialkyl amino, such as aminoisobutyric acid (Aib) acids, would severely restrict the Φ and Ψ torsion angles of that residue to those associated with right- or left-handed helices (both α- and 3_{10}-helices). Subsequent experimental validation of that prediction is abundant.[7] Alternatively, the helical structure can be stabilized through the incorporation of covalent or noncovalent linkages between side chains of two residues separated in sequence, but spatially close in a helix, such as residues *i* and $i + 4$ of an α-helix. Examples of chemical linkages shown to enhance helical propensity include salt bridges, hydrophobic interactions, aromatic–charge or aromatic–sulfur interactions, disulfide bonds, lactam bridges, hydrocarbon staplings, diaminoalkanes, acetylenes, and metal ligation between natural and unnatural amino acids (for a recent review, see Che et al.[5] and references therein). Helical peptides are stabilized by extensive, but weak intrachain H-bonds; design of covalent mimics of intrachain H-bonds reinforces the helical structure.[8,9] Though the main body of a peptide helix is stabilized by intrachain H-bonds, free NH groups at the N-terminus and CO groups at the C-terminus of the helix cannot participate in such internal H-bonding. Thus, preorganized helix-nucleating templates[10,11] have been developed in which the orientation of the first 4 NH groups or the last 4 CO groups is fixed in a rigid structure to template helix formation and prevent fraying of either end.

Alternatively, unnatural oligomers with a strong tendency to adopt helical conformation have also been described to target helix-recognition surfaces. Many of these are structural variants of polypeptides that are essentially stable to most proteases. One such family of oligomers is the poly-*N*-substituted glycines or "peptoids"[12] on which the amino-acid side chains are appended to amide nitrogens rather than to the α-carbons. Despite the achirality of the *N*-substituted glycines backbone and its loss of amide H-bond donors, peptoids containing α-chiral, sterically bulky side chains are able to adopt stable, chiral helices with *cis*-amide bonds. The periodicity of the peptoid helix is three residues per turn, with a pitch of 6 Å.[13] The other family is the β-peptides,[14,15] which differ from α-peptides by one additional backbone carbon atom between the amino and carboxyl groups. β-peptides composed of β^3-$_L$-amino acids are able to form left-handed 14-helices characterized by a periodicity of three residues per turn with a pitch of 4.7 Å and H-bonds between the backbone amide proton of residue *i* and the carbonyl oxygen of residue $i + 2$. The ability to form stable helices makes peptoids and β-peptides good candidates for mimicry of bioactive peptides that rely on helical structure for molecular recognition.[16–18] Alternative helical structures of regular and hybrid peptides consisting of homologous amino acids, such as β-, γ-, and δ-amino acids, have been explored and shown to inhibit helix recognition.[19–22]

Since the critical surface for α-helix recognition often involve the side chains of residues *i*, $i + 3$ and/or $i + 4$, and $i + 7$, along one face of the α-helix, one can design appropriate scaffolds with limited conformations to orient attached functional groups that closely resemble the surface of α-helices. There are 3.6 residues per turn of an α-helix, with a rise of 1.5 Å per residue. The characteristic axial rise between these four key residues is 4.5 or 6.0 Å, respectively (see Figure 1). Looking down the helical axis, residues are projected at -60° and 40° for $i \rightarrow i + 3$ and $i \rightarrow i + 4$ interactions, respectively. Hamilton and coworkers[23–27] described a terphenyl scaffold that can reasonably imitate side-chain orientations seen in α-helices in which the 3,2′,2″-substituents on the phenyl rings present functionalities in a spatial relationship that mimics the *i*, $i + 3$ or $i + 4$, and $i + 7$ residues on an α-helix. Comparing the ideal α-helical structure and the terphenyl scaffold, when the terphenyl is in a staggered conformation with $\omega_1 = -60^\circ$ and $\omega_2 = 40^\circ$, the three substituents project from the terphenyl core with similar angular relationships and 5–30% shorter distances in the characteristic rise corresponding to $i \rightarrow i + 3$ and $i \rightarrow i + 4$ interactions in a native helix, respectively; similarly, when the terphenyl scaffold adopts another staggered conformation with $\omega_1 = 40^\circ$ and $\omega_2 = -60^\circ$, the three substituents correspond better to the *i*, $i + 4$, and $i + 7$ positions. Proofs of concept for helix mimetics in protein–protein recognition came from successfully disrupting the interaction between calmodulin and an α-helical domain of smooth muscle light-chain kinase[23]; inhibiting the assembly of HIV gp41, thereby, reducing levels of viral entry into host cells[24]; preventing the interaction between the proapoptotic protein Bak and the antiapoptotic protein Bcl-x_L[25,26]; and blocking the complex formation of the tumor-suppressor p53 with the oncoprotein HDM2.[27]

Compared to other templates containing a chiral axis, the terphenyl is a typical drug-like scaffold. In a retrospective analysis[28] of privileged structures of pharmacologically active

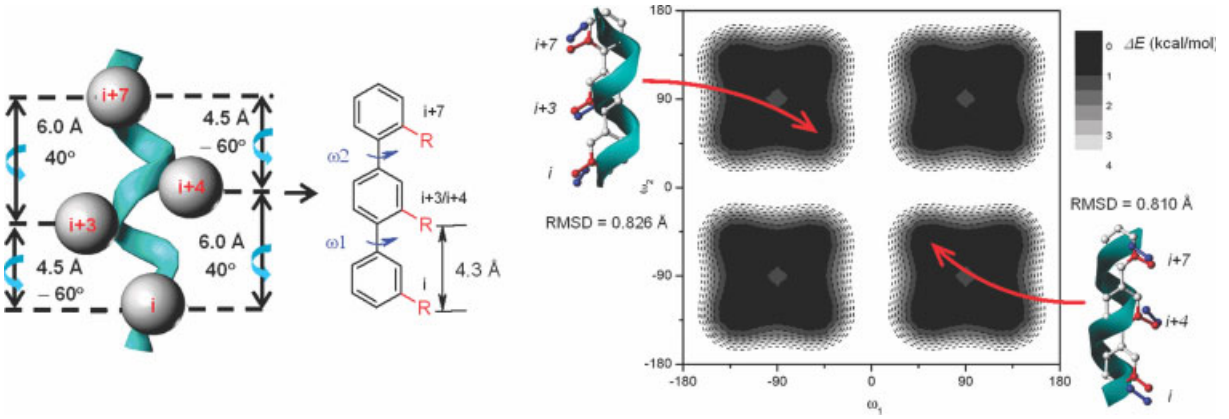

FIGURE 1 (Left) The idealized α-helix geometry with 4.5 or 6.0 Å rise between residues i, $i + 3$, $i + 4$, and $i + 7$ and the tris-substituted terphenyl as a prototype of α-helix mimetic. (Right) The potential energy surface of the tris-substituted terphenyl (R = Me) determined at the B3LYP/6-31G* level of theory. The trimethyl substituents (colored in red) are superimposed with the C_α—C_β bonds (colored in blue) of an ideal α-helix. The RMSD for C_α—C_β bonds for the two preferred staggered conformations of the terphenyl were 0.826 and 0.810 Å, respectively.

compounds, biaryls were found to be present in 7.4% of reference drug molecules. The terphenyl and its derivatives represent, therefore, an attractive means to modulate helix-recognition function and to enlarge the scope of peptidomimetic scaffolds. However, the terphenyl scaffold is not rigid; for example, it adopts both right- and left-handed twists. Our previous studies indicated that there were 16 energetically almost equal conformers, only two of which could mimic either of the desired helical side-chain orientations. Thus, the terphenyl scaffold is not optimally preorganized in terms of α-helical mimicry due to its conformational heterogeneity. Here, we computationally engineered and evaluated various organic scaffolds to determine how well they can orient side chains in positions corresponding to side chains of α-helices. One aspect of scaffold selection was the amount of correct preorganization introduced by the scaffold versus alternative conformations. In addition, we examined the impact of the scaffold itself on the distribution of side-chain rotamers. Further, we described metal-complexes of helix mimics as a logical extension for the mimicry of different helix–helix packing motifs.

COMPUTATIONAL METHODS

The geometries and the potential energy surfaces of considered compounds were optimized and explored with the Gaussian 03 program using density functional calculations at the B3LYP/6-31G* level of theory. The conformation of the terphenyl and its derivatives can be described with two torsion angles, ω_1 and ω_2, of the two bonds connecting the adjacent aromatic rings. The ω-angle energy profile usually led to a double minimum potential between 0° and 180°. Here, the syndiagonal one ($0^\circ < \omega < 90^\circ$) is denoted as "syn" and the antidiagonal form ($90^\circ < \omega < 180^\circ$) is referred as "anti." One aspect of the design was trying to stabilize the syn form relative to the anti one [$\Delta E^\alpha = E^{syn} - E^{anti}$]; and the other aspect was to lower the rotational barriers at $\omega = 0^\circ$ [$\Delta E^0 = E^0 - E^{syn}$] and $\omega = 90^\circ$ [$\Delta E^{90} = \Delta E^{90} - E^{syn}$] to allow facile interconversion among conformations necessary for an induced fit upon binding to a receptor. The impact of aqueous solution on conformational preferences was considered by single-point energy calculation with the polarizable continuum model. Generally, the impact of water was relatively minor; the results were summarized in Supplementary Tables S1 and S2.

Several force fields (MM2*, MM3*, AMBER*, OPLSAA, and MMFF) were also examined with these compounds. Generally, the DFT results favor MM2* as having the more compatible parameters for this series. This has led us to use MM2* for a qualitative comparison of the conformational preference of the terphenyl scaffold with those of other scaffolds and the distributions of side-chain rotamers on these templates. These exploratory studies were done with mixed Monte Carlo/stochastic dynamics (MC/SD) simulations. The simulations were carried out at 300 K using the MM2* force field with the GB/SA salvation model for water as implemented in MacroModel 9.1. A time step of 0.5 fs was used for the SD part of the simulation. The MC simulation used random torsional rotation between ±90° and ±180° for ω_1 and ω_2, and between ±60° and ±180° for χ_1. Other spaces were effectively sampled through the SD part of the simulation. The total simulation time was 5 ns for each compound under investigation, and samples were taken at 1 ps intervals, yielding 5000 conformations for analysis.

RESULTS AND DISCUSSION

Conformational Restriction

The twist angles of terphenyls, ω_1 and ω_2, are balanced by two competing factors of approximately the same order of

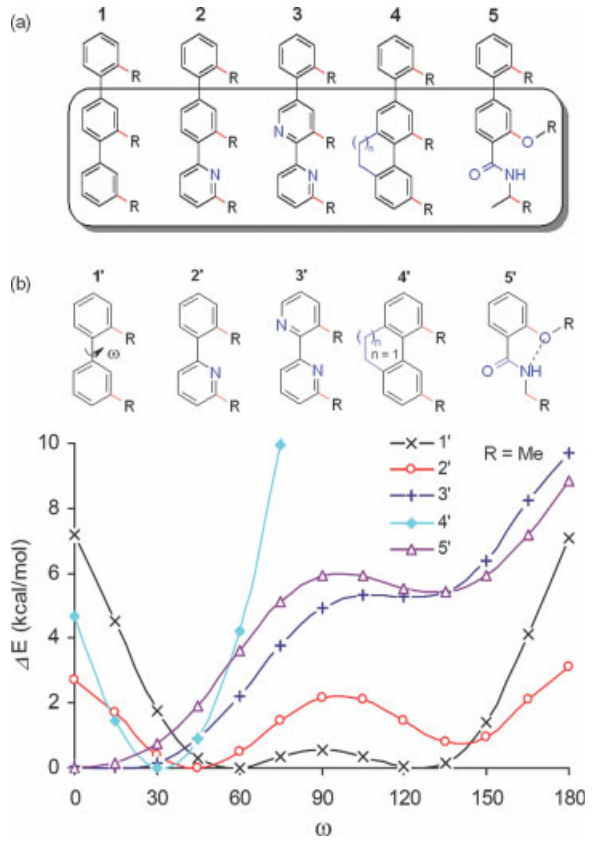

FIGURE 2 (a) Terphenyl (**1**) and conformationally constrained helix mimetics (**2**–**5**) with one rotation angle restricted by different mechanisms: steric repulsions (**2**–**3**), covalent linkages (**4**) and H-bonds (**5**), and (b) the relative energy (kcal/mol) as a function of ω-angle for the corresponding biaryl analogs (**1′**–**5′**) determined at the B3LYP/6-31G* level of theory.

magnitude, namely the electron delocalization between the π orbitals of the adjacent aryl rings and the steric repulsion between *ortho*-H-atoms and other substituents. Electron delocalization prefers a coplanar arrangement, while steric interactions force the molecule to be nonplanar; and the balance of these two results in staggered, or twisted, structures. DFT calculations on substituted terphenyl **1** showed that there were 16 energetically almost equal conformers, and among them only two could mimic the desired α-helical twist. One staggered structure with $\omega_1 = -55.7^\circ$ and $\omega_2 = 55.6^\circ$ is able to project substituents with a close correspondence of the side-chain positions of residues (i, $i + 3$, $i + 7$) of an ideal α-helix with root mean square displacement (RMSD) on C_α—C_β bonds of 0.826 Å. The other staggered conformer with a set of mirrored twist angles of $\omega_1 = 55.7^\circ$ and $\omega_2 = -55.6^\circ$ can mimic the side chains of residues (i, $i + 4$, $i + 7$) with a similar RMSD of 0.810 Å. In addition, the relative low energy barrier of rotation of the aryl–aryl single bonds, $\Delta E^0 = 7.21$ and $\Delta E^{90} = 0.55$ kcal/mol, should enable facile interconversion among the 16 possible twisted conformers at room temperature.

In order to stabilize the syn form and to augment the helix-mimicry propensity, several approaches to chemically engineer terphenyls were examined, including the use of steric repulsion, covalent linkages, and H-bonds, as illustrated in Figure 2. In the following, the corresponding biaryl analogs were used to discuss and compare the impact of different restriction factors on the rotation around the aryl–aryl single bond. The DFT results are summarized in Figures 2 and 3 and Tables I and II, and the impact of water on conformational preferences is included in the supplementary information.

(1) Replacing the phenyl ring with a pyridyl group leads to a less twisted structure due to a weaker repulsion between the nitrogen lone pair and the H-atom compared to the

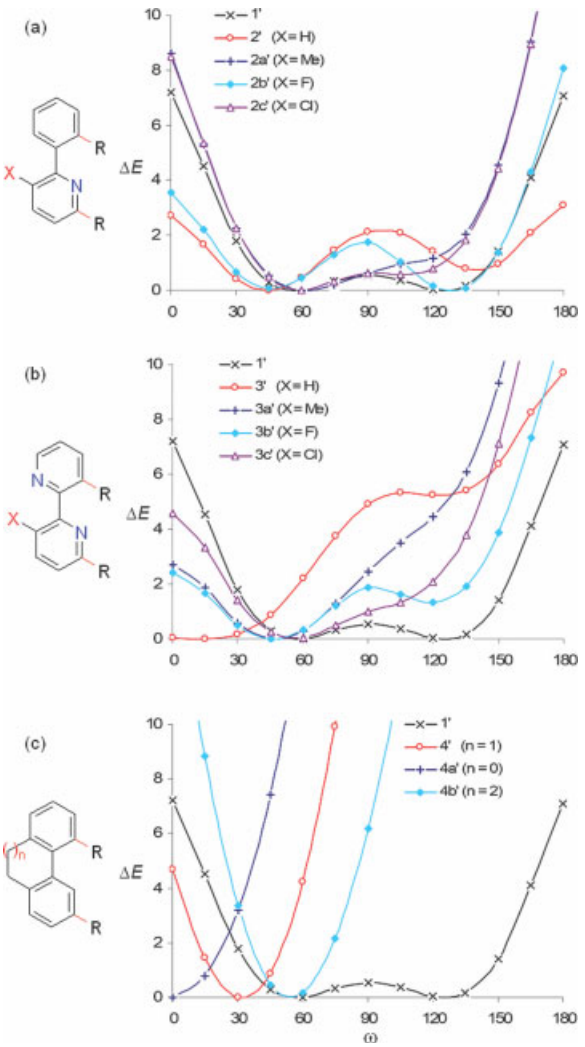

FIGURE 3 The relative energy (kcal/mol) as a function of ω-angle for substituted biphenyl (**1′**) and its conformationally constrained analogs (**2a′**–**2c′**, **3a′**–**3c′**, and **4a′**–**4b′**) determined at the B3LYP/6-31G* level of theory.

Table I Torsional Angles, Syn–Anti Energy Differences, and Rotational Barriers Through ω = 0° and 90° for Substituted Biphenyl and its Conformationally Constrained Analogs (1′–5′) Determined at the B3LYP/6-31G* Level of Theory

	ω (syn)	ΔE^{α}	ΔE^{0}	ΔE^{90}
1′	57.1°	0.01	7.21	0.55
2′	43.7°	−0.74	2.71	2.15
3′	17.4°	−5.25	0.03	4.91
4′	32.1°	–[a]	4.68	17.68
5′	2.1°	−5.42	0.00	5.94

[a]A single-minimum potential energy surface.

interaction between two H-atoms. The syn conformer of **2′** was favored both *in vacuo* and in water. DFT-optimized structure of **2′** was shown to have a global minimum at $\omega =$ 43.7° of the syn form and a local minimum at $\omega = 140.3°$ of the anti form, which is 0.74 kcal/mol higher in energy. The two substituents project from **2′** with closer angular relationship corresponding to the $i \rightarrow i + 4$ interaction in an ideal α-helix than those of substituted biphenyls. The calculations also suggested that the rotational barrier at 0° was 2.71 kcal/mol, significantly lower than those of substituted biphenyls, while the barrier at 90° was 2.15 kcal/mol, higher than those of biphenyls. Both of the rotational barriers were slightly reduced in water. These indicated that thermal energy would enable more facile interconversion among the 16 possible twisted conformers of pyridine-derived helix mimetics than those of terphenyls at room temperature.

Similarly, substitution of the *ortho*-H-atom on the opposite side of the aryl ring by a larger atom (such as halogens) or group (such as methyl), could further stabilize the syn conformer and modulate the twist angles and rotational barriers (Figure 3a: **2a′**–**2c′**). For **2a′** (X = Me), a single minimum potential was determined, with the "anti" minimum having disappeared. So, the syn form was dominant in **2a′** with a twist angle of 61.5°. The rotational barrier at 0° was 8.63 *in vacuo* and 8.35 kcal/mol in water, which should still allow relatively easy interconversion among all syn conformations. Fluorine has a similar van der Waals radius (1.35 Å) compared to that of hydrogen (1.20 Å), but a much stronger electronegativity. For **2b′** (X = F). The calculations indicated that the syn conformer was 0.09 and 0.65 kcal/mol less stable than the anti structure *in vacuo* and in water, respectively. On the other hand, chlorine has a larger van der Waals radius (1.75 Å) similar to a methyl group. Thus, for **2c′** (X = Cl), the syn structure was favored by 0.58 kcal/mol *in vacuo* and 0.18 kcal/mol in water, respectively.

(2) Replacing both phenyl groups with pyridyls, as in analog **3**, resulted in an almost coplanar structure due to reduced steric repulsion along both sides of the scaffold. For the substituted bipyridine, **3′**, DFT calculations revealed a global minimum in the syn conformation with a twist angle of 17.4° and a local minimum at 124.0° of the anti form, which were 5.25 and 1.95 kcal/mol higher in energy *in vacuo* and in water, respectively. Therefore, the syn conformation of **3′** was clearly dominant. Further, the rotational barrier at 0°, 0.03 kcal/mol *in vacuo* and 0.19 kcal/mol in water, can essentially be neglected.

Introducing another steric factor, through the substitution of the *ortho*-H-atom on the opposite side of the pyridyl with a larger atom or group, can effectively adjust the twist conformations and the syn–anti energy differences (Figure 3b: **3a′**–**3c′**). For **3a′** (X = Me), similar to **2a′**, due to the strong repulsion between two methyl groups, led to a single minimum potential, with the "anti" minimum vanished from the potential-energy surface. The syn conformer has a twist angle of 46.9°, and significantly lower rotational barrier at 0° of 2.71 and 3.38 kcal/mol *in vacuo* and in water, respectively. For **3b′** (X = F), the syn conformation was preferred *in vacuo* by 1.32 kcal/mol; however, in water the syn structure was 0.34 kcal/mol less stable than the anti one. Such a modification might be less suitable for helix mimicry. For **3c′** (X = Cl), it also had a single minimum potential, showing a syn structure with a twist angle of 56.2°. Thus, **3c′** has a similar energy profile and shows similar conformational behavior to **3a′**.

(3) Alternatively, the syn structure can be stabilized through the incorporation of covalent linkages between adjacent aryl rings. One example is the C—C single bond, as in analog **4**, which effectively locks the scaffold in the syn conformation and may also afford enhanced biostability. For the model compound **4′** ($n = 1$), DFT calculations revealed only one minimum at $\omega = 32.1°$ of the syn form and a rotational barrier at 0° of 4.68 and 4.39 kcal/mol *in vacuo* and in water, respectively. The anti structures could be largely ignored due to the large transition barrier at 90°.

Table II Torsional Angles, *Syn–Anti* Energy Differences, and Rotational Barriers for Conformationally Constrained Analogs Determined at the B3LYP/6-31G* Level

		ω (syn)	ΔE^{α}	ΔE^{0}	ΔE^{90}
2a′	X = Me	61.5°	–	8.63	0.61
2b′	X = F	45.4°	0.09	3.55	1.74
2c′	X = Cl	59.5°	−0.58	8.51	0.61
3a′	X = Me	46.9°	–	2.71	2.46
3b′	X = F	46.0°	−1.32	2.42	1.88
3c′	X = Cl	56.2°	–	4.60	0.99
4a′	$n = 0$	0.3°	–	0.00	33.50
4b′	$n = 2$	54.3°	–	16.72	6.18

Varying the length of the carbon–carbon constraints provided another means of adjusting the twist angles and the rotation barriers (Figure 3c: **4a′** and **4b′**). In general, the rotational energy profiles as functions of ω-angles for all three constrained templates (**4′**, **4a′**, and **4b′**) were similar in shape. For the smaller C—C bond constrained analog **4a′** ($n = 0$), the profile shifted to the left and led to a preferred coplanar conformation ($\omega = 0.3^\circ$). While for the larger constrained analog **4b′** ($n = 2$), the profile shifted to the right and resulted in a twisted structure with $\omega = 54.3^\circ$; however, it also led to an insuperable barrier at 0° at room temperature, which suggests that the incorporation of more than three C—C single bond constraint is less useful for helix mimicry.

(4) The incorporation of noncovalent linkages, such as H-bonds, should also maintain the similarity between the arrangement of the key residues of an α-helix and the substituents on the new template **5**, while increasing the rigidity of the scaffold. This strategy was previously demonstrated by Hamilton and coworkers[29] using terephthalamide as the scaffold. The flanking phenyl ring in the terphenyl was replaced by a functionalized carboxamide group, which still retained the planar geometry of the phenyl ring, due to the restricted rotation of the amide bond. The new conformational constraint in the molecule was imposed by an intramolecular H-bond between the amide NH group and the alkoxy oxygen atom, to influence the position of the functional group. Our DFT calculations on the model compound **5′** showed that the newly introduced carboxamide group led to a coplanar syn structure at $\omega = 2.1^\circ$ and a twist anti conformer at $\omega = 131.2^\circ$, which was 5.42 and 2.81 kcal/mol higher in energy *in vacuo* and in water, respectively. Both rotational barriers at 0° and 90° were relatively small, of 0 and 3.75 kcal/mol in water, suggesting that both syn and anti conformations would be present with the coplanar syn conformation being favored. This was consistent with NMR studies[29] that indicated that 72% of a terephthalamide derivative adopted the syn conformation in chloroform.

The Terpyridyl Scaffold

The design of a next generation of α-helix mimetics should provide a relatively rigid preorganized framework from which side chains are projected in such a way to resemble those key residues closely. Other criteria for mimetic design include a modular synthesis and moderate aqueous solubility. Based on the above arguments, a terpyridyl scaffold[1,30] had been designed as an improved α-helix mimetics. The terpyridyl scaffold assumes a preferred conformation in which all three substituents are projected to the same face of the molecule and augments the propensity in α-helix mimicry through unbalanced steric interactions. The canonical ensembles of the substituted terphenyl and terpyridyl were obtained from mixed MC/SD simulations done with the MM2* force field and the GB/SA water model, as illustrates in Figure 4. It was estimated, for the terphenyl scaffold, that only about 7.1%, slightly more than one sixteenth (6.25%), of the whole ensemble exhibits the characteristic orientations of amino acid side chains i, $i+3$ and $i+7$, ($-90^\circ < \omega_1 < 0^\circ$, $0^\circ < \omega_2 < 90^\circ$) or side chains i, $i+4$, and $i+7$ ($0^\circ < \omega_1 < 90^\circ$, $-90^\circ < \omega_2 < 0^\circ$) of an α-helix. These suggested that the terphenyl scaffold was limited in terms of α-helical mimicry due to its conformational heterogeneity. Thus, a helical peptidomimetic with biological activity based on the terphenyl derivative would still be ambiguous with regard to determination of the receptor-bound conformation in the absence of crystal structure or NMR data of the complex. On the other hand, the terpyridyl scaffold is much more rigid and limits side-chain orientations to a greater extent than does the terphenyl. The percentage of the time that the (i, $i+3$, $i+7$) or (i, $i+4$, $i+7$) orientation of side chains would be populated has risen to 17.2% of the time, more than twice that of the terphenyl. Further, the newly introduced pyridyls also increase aqueous solubility. Our tentative conclusion is that the terpyridyl scaffold should be superior as a α-helix mimetics as reflected in enhanced binding affinity due to lower loss of entropy on binding through preorganization.

(i, $i+3$, $i+7$) and (i, $i+4$, $i+7$) Selective α-Helix Mimetics

The characteristic axial rise between substituents of terphenyls is 4.3 Å which is 5% shorter than that of the $i \rightarrow i+3$ geometry in a native α-helix and 30% shorter than that of the $i \rightarrow i+4$ interaction. Such arrangement cannot effectively differentiate between the specific recognition through side chains of residues (i, $i+3$, $i+7$) with that of residues (i, $i+4$, $i+7$), due to the freely rotatable aryl–aryl single bonds. Here, we discuss three modifications (Figure 5 and Table III) in order to improve the current design to selectively resemble the spatial relationship of side chains of residues (i, $i+3$, $i+7$) or that of residues (i, $i+4$, $i+7$), or even all four side chains along one face of an α-helix.

(1) To shift one substituent one single bond away from others along the axis will increase one of the characteristic axial rise to 6.5 Å, very close to the $i \rightarrow i+4$ geometry in a native α-helix. Further, to move the substituent another single bond from the axis will keep all three substituents pointing toward the same direction as observed in α-helical structures. To overcome the steric repulsion between the substituent and the anchor aryl ring, which forces the substituent to

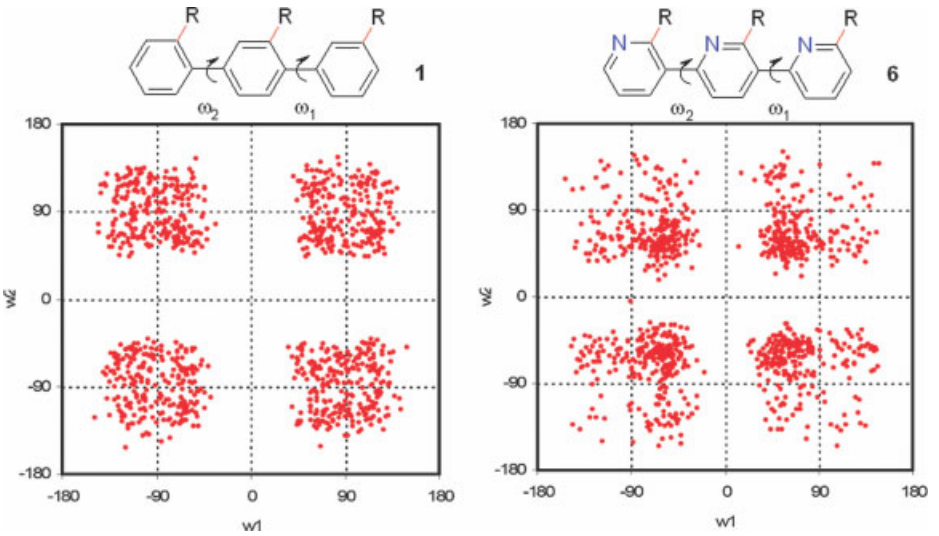

FIGURE 4 The canonical ensemble of the 3,2′,2″-tris-substituted-terphenyl scaffold (**1**, left) and the 6,6′,2″-tris-substituted-2,4′:2′:3″-terpyridyl scaffold (**6**, right) obtained from mixed MC/SD simulations done with the MM2* force field and the GB/SA water model.

tilt away from the desired twist angle, a new aryl ring is required, such as the use of naphthalene. Depending upon the position of the naphthalene and the site of the substituent, newly designed templates can selectively resemble the spatial relationship of side chains of residues (i, $i + 3$, $i + 7$), such as **7** and **8**, or residues (i, $i + 4$, $i + 7$), such as **11** and **12**, of an α-helix, respectively. DFT-optimized structures suggested that RMSDs on the C_α—C_β bonds were between 0.492 and 0.653 Å, an improvement compared to those of terphenyls, which were about 0.810–0.826 Å. In addition, the naphthalene can be replaced with an isosteric group, such as benzamide, will also allows to selectively orient the substituents in space to closely mimic side chains of residues (i, $i + 3$, $i + 7$), such as **9** and **10**, or residues (i, $i + 4$, $i + 7$), such as **13**

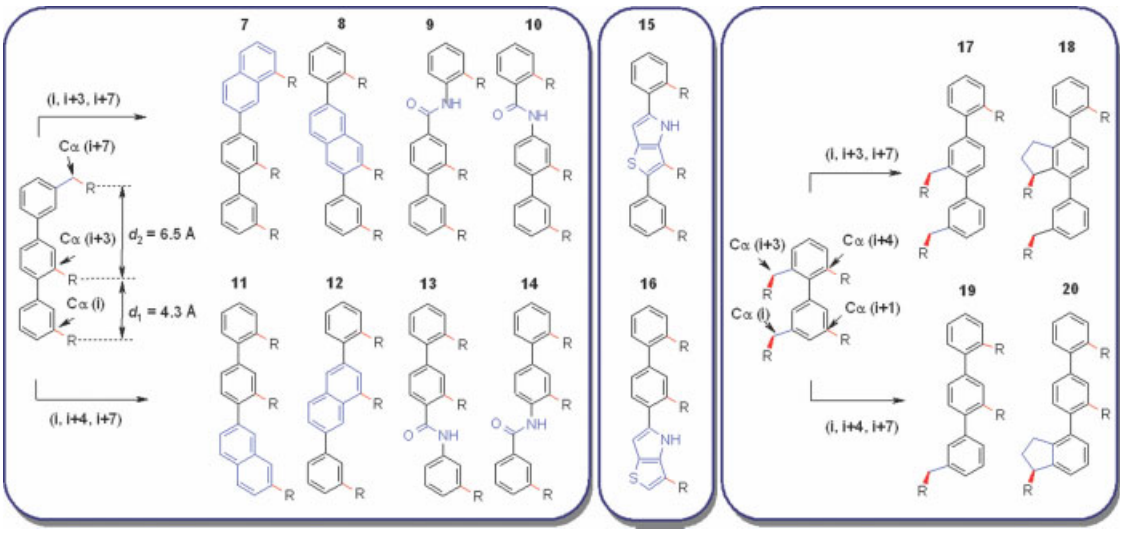

FIGURE 5 α-Helix mimetics designed to selectively resemble the orientation of side chains (i, $i + 3$, $i + 7$) or side chains (i, $i + 4$, $i + 7$): (left) to shift one substituent along the axis increases one characteristic axial rise to 6.5 Å, close to the $i \rightarrow i + 4$ geometry; (middle) the incorporation of appropriate polycyclic rings, such as thieno[3,2-*b*]pyrrole, has a similar effect; (right) the extension of a methyl (to become an ethyl) can expand the scaffold to resemble the orientation of both side chains of residues i and $i + 1$ in a single aryl unit. Adapted from Che et al., J Comput Aided Mol Des 2006, 20, 109–130.

Table III Selected Geometrical Parameters of DFT-Optimized (B3LYP/6-31G*) Structures and RMSD Overlay of α-Helix and Designed α-Helix Mimetics

		α-helix: (i, $i+3$, $i+7$)					α-helix: (i, $i+4$, $i+7$)			
		ω_1 (°)	ω_2 (°)	d_2 (Å)	RMSD (Å)		ω_1 (°)	ω_2 (°)	d_1 (Å)	RMSD (Å)
A	**7**	−55.4	37.2	6.5	0.540	**11**	53.8	−55.3	6.5	0.653
	8	−61.1	54.6	6.5	0.639	**12**	38.0	−57.3	6.5	0.492
	9	−55.9	26.8	6.1	0.444	**13**	41.8	−55.5	6.1	0.602
	10	−55.4	43.5	6.1	0.555	**14**	26.7	−55.0	6.1	0.591
B	**15**	−44.0	40.5	5.9	0.612	**16**	39.2	−54.5	5.9	0.589
C	**17**	−64.5	18.3	5.4	0.644	**19**	20.3	−55.0	5.4	0.569
	18	−72.3	55.8	5.5	0.697	**20**	40.4	−55.9	5.5	0.442

and **14**. DFT studies indicated that RMSDs on the C_α—C_β bonds were between 0.444 and 0.602 Å, better than naphthalene-based helix mimetics. Further, benzamide derivatives are more soluble and can be prepared by simple amide formation. In addition, the amide group, connecting adjacent aryl rings, can be switched to the opposite direction to enlarge current design for better structures with improved physicochemical properties.

(2) Similarly, the incorporation of appropriate bicyclic aryl rings, such as the substituted thieno-[3,2-b]-pyrrole or furo-[3,2-b]-pyrrole as exemplified in Figure 6, will also increase one characteristic axial rise to 5.9 Å, suggesting that one can reposition substituents to more closely resemblance of the $i \rightarrow i+4$ geometry of an ideal α-helix. Placing the bicyclic aryl ring in the middle or at one end of the template can allow the mimetics to present attached functional groups to selectively imitate the orientation of side chains of residues (i, $i+3$, $i+7$), such as **15**, or residues (i, $i+4$, $i+7$), such as **16**, of a native α-helix. RMSDs on the C_α—C_β bonds were 0.612 and 0.589 Å for DFT-optimized structures, **15** and **16**,

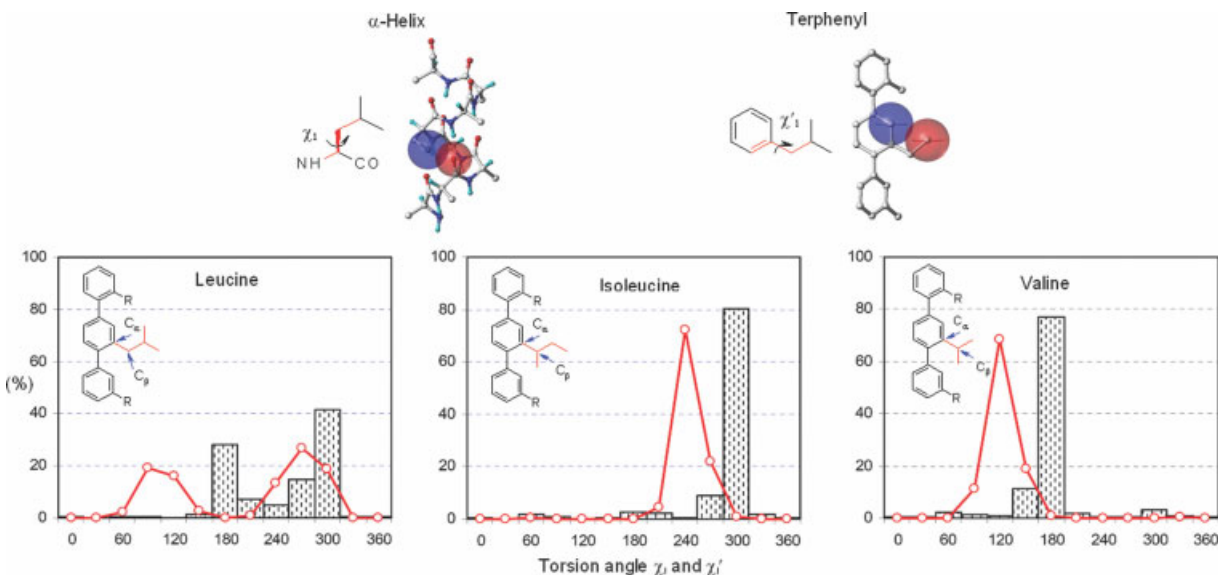

FIGURE 6 Histogram of side-chain rotamers, χ_1 (filled bars), observed for Leu, Ile and Val residues in the α-helical conformation from high resolution crystal structures, and comparison with those distribution in the terphenyl derivatives, χ_1'(red lines), as the terphenyl axis is aligned with the helix axis. (Note: if the terphenyl axis is superimposed upon the α-helix axis, χ_1' and χ_1 have the following relationship, $\chi_1 \approx \chi_1 + 5°$). The rotamer distribution of terphenyl derivatives was estimated using the mixed MC/SD simulations done with the MM2* force field and the GB/SA water model (R = Me). In α-helices, the g^+ rotamer of angle χ_1 is almost forbidden because any side chain would overlap atoms of the previous turn of the helix; while, in terphenyls, the side-chain orientation is also restricted due to steric repulsion with *ortho*-carbons on the same aryl ring. Adapted from Che et al., J Comput Aided Mol Des 2006, 20, 109–130.

aligned with those of an α-helix. Therefore, such modification showed a 25% improvement in the optimization of RMSDs compared to terphenyls.

(3) On the basis of the semiempirical calculations, Jacoby[31] proposed that 2,6,3′,5′-substituted biphenyls as α-helix mimetics superimposing the side chains of residues *i*, *i* + 1, *i* + 3, and *i* + 4, with an RMSD on C_α—C_β bonds of 0.47 Å. Thus, this opens the possibility to selectively mimic side chains of residues (*i*, *i* + 3, *i* + 7) or residues (*i*, *i* + 4, *i* + 7), or even all critical residues along one face of an α-helix with terphenyl derivatives. For example, one subset of such modifications, **17** and **19**, can superimpose the side chains of residues (*i*, *i* + 3, *i* + 7) and residues (*i*, *i* + 4, *i* + 7) with RMSDs of 0.644 and 0.569 Å, respectively. In addition, Horwell et al.[32] also demonstrated that 1,6-disubstituted indanes present functionality in a similar spatial arrangement to the *i* and *i* + 1 residues of an α-helix. Therefore, the incorporation of substituted indanes[33] at different positions in the template provides a nice way to rigidify the scaffold, while at the same time present critical recognition functionality in a suitable spatial orientation as in a native α-helix for binding to a receptor. For example, the introduction of substituted indanes into **17** and **19** leads to more rigid analogs **18** or **20**, which show similar RMSDs of 0.697 and 0.442 Å, respectively.

We believe that the combination of these chemical modifications within the original terphenyls can lead to better helix mimetics showing closer mimicry of the spatial arrangement of side chains of a native α-helix, more rigid template structures, and better physicochemical properties. These make a general approach possible to helix-mimetic scaffolds that can be targeted for multiple therapeutic applications by simple changing the nature of the side-chain substituents.

Side-Chain Rotamers

An equally important consideration for the design of peptidomimetics is the side-chain orientation beyond the C_α—C_β bonds. Generally, rotations about the bonds of amino acid side chains (χ_1, χ_2, and etc) are close to one of the three conformations (*t*, g^+, and g^-) in which the attached atoms on the bond are staggered, with the conformation that gives the largest separation of the bulkiest groups being favored. In α-helices, the side chains project outward into solution, although they are tilted toward the amino end of the helix and need not interfere with the helical backbone. There are, however, varying restrictions on conformation of the side chains. In particular, the g^+ rotamer of angle χ_1 between the C_α and C_β is almost forbidden because any side chain would overlap atoms of the previous turn of the helix. Side chains with branched C_β atoms (Val, Ile, and Thr) are most restricted in their conformations. This rationalizes the characterization of Val, Ile, and Thr as "helix breakers."[34] The distribution of side-chain rotamers of angle χ_1 in a database of α-helical structures has been examined.[35] Three classes of distribution were found that differ in the relative population between *t* and g^- rotamers (see Figure 6). For side chains without branched C_β atoms, such as Leu, both of the *t* and g^- rotamers are somewhat equally populated. For the side chains of Ile and Thr, each has a center of asymmetry at C_β, which leads to a prominent peak centered at the g^- rotamer. To the contrary, the side chain of Val, without an asymmetry center at C_β, shows a dominant preference for the *t* rotamer.

Similarly, χ_1' is defined as the torsion angle around the corresponding C_α—C_β bond on terphenyls. If the terphenyl axis is superimposed upon the α-helix axis, angles χ_1' and χ_1 are close in values ($\chi_1' \approx \chi_1 + 5^\circ$). The distribution of angle χ_1' was obtained from canonical ensembles of substituted terphenyls determined with mixed MC/SD simulations using the MM2* force field and the GB/SA water model. Three representative distributions for substituted terphenyls are shown in Figure 6 in comparison with those of α-helical structures. The study revealed that the terphenyl template also restricted side-chain orientations due to the steric repulsion with *ortho*-carbons on the same aryl ring. This leads to an unfavorable structure when the corresponding C_γ atom sitting on the same plane of the anchoring aryl ring. Inspection of the pattern of angle χ_1' indicated that the distributions of side-chain rotamers were similar in shape compared to those of α-helices, except that the profiles of angle χ_1' consistently showed an approximately 60°-shift (to a smaller value). This may in part explain why those analogs with the highest affinity for helix-recognition sites differ in side-chain substituents between the native helices and the helical mimetics. Determination of the 3D structures of helix mimetics bound with receptors and comparison with α-helical recognition motifs has not been yet reported.

CONCLUSIONS

Peptides are applied therapeutically to only a limited extent because of undesirable absorption, distribution, metabolism and excretion (ADME) properties, undesired side effects due to undesirable interactions of conformationally flexible peptides with nontargeted receptors. This led to the concept of peptidomimetics, nonpeptidic compounds that imitate the structure of a peptide in its receptor-bound conformation. For modulating protein–protein interactions, general approaches for mimicking protein surfaces with small molecules represent a significant advance. In this study, we described novel α-helix mimetics which are more effective

than current scaffolds at constraining the aryl–aryl torsion angles to those associated with α-helical twists and can selectively superimpose the side chains of residues *i*, $i + 3$ or $i + 4$, $i + 7$ with an improved RMSD of approximately 0.5 Å. In addition, our studies uncovered the limitation of using these polyaromatic scaffolds to imitate side-chain orientations of an α-helix beyond C_β atoms. The distributions of side-chain rotamers around the C_α—C_β bonds of the terphenyl derivatives are similar in shape, but with an approximately 60°-shift, compared to those of α-helices. Knowing that molecular recognition of most, if not all, protein–protein interactions involve helix recognition, the scaffolds examined should be useful in the design of novel helix mimetics as structural elements in nanotechnology and protein engineering, as pharmacological probes, and as potential therapeutic agents.

YC acknowledges a research fellowship from the National Heart, Lung and Blood Institute.

REFERENCES

1. Che, Y. Molecular Biophysics; Washington University: St. Louis, MO, 2003; pp 1–208.
2. Mammen, M.; Shakhnovich, E.; Whitesides, G. M. J Org Chem 1998, 63, 3168–3175.
3. Searle, M. S.; Williams, D. H. J Am Chem Soc 1992, 114, 10690–10697.
4. Marshall, G. R.; Head, R. D.; Ragno, R. Thermodynamics in Biology; Di Cera, E., Ed.; Oxford University Press: Oxford, 2000; pp 87–111.
5. Che, Y.; Brooks, B. R.; Marshall, G. R. J Comput Aided Mol Des 2006, 20, 109–130.
6. Marshall, G. R.; Bosshard, H. E. Circ Res 1972, 31, 143–150.
7. Marshall, G. R.; Hodgkin, E. E.; Langs, D. A.; Smith, G. D.; Zabrocki, J.; Leplawy, M. T. Proc Natl Acad Sci USA 1990, 87, 487–491.
8. Cabezas, E.; Satterthwait, A. C. J Am Chem Soc 1999, 121, 3862–3875.
9. Chapman, R. N.; Dimartino, G.; Arora, P. S. J Am Chem Soc 2004, 126, 12252–12253.
10. Kemp, D. S.; Boyd, J. G.; Muendel, C. C. Nature 1991, 352, 451–454.
11. Austin, R. E.; Maplestone, R. A.; Sefler, A. M.; Liu, K.; Hruzewicz, W. N.; Liu, C. W.; Cho, H. S.; Wemmer, D. E.; Bartlett, P. A. J Am Chem Soc 1997, 119, 6461–6472.
12. Simon, R. J.; Kania, R. S.; Zuckermann, R. N.; Huebner, V. D.; Jewell, D. A.; Banville, S.; Ng, S.; Wang, L.; Rosenberg, S.; Marlowe, C. K.; Spellmeyer, D. C.; Tan, R. Y.; Frankel, A. D.; Santi, D. V.; Cohen, F. E.; Bartlett, P. A. Proc Natl Acad Sci USA 1992, 89, 9367–9371.
13. Armand, P.; Kirshenbaum, K.; Goldsmith, R. A.; Farr-Jones, S.; Barron, A. E.; Truong, K. T. V.; Dill, K. A.; Mierke, D. F.; Cohen, F. E.; Zuckermann, R. N.; Bradley, E. K. Proc Natl Acad Sci USA 1998, 95, 4309–4314.
14. Gellman, S. H. Acc Chem Res 1998, 31, 173–180.
15. Seebach, D.; Kimmerlin, T.; Sebesta, R.; Campo, M. A.; Beck, A. K. Tetrahedron 2004, 60, 7455–7506.
16. Hara, T.; Durell, S. R.; Myers, M. C.; Appella, D. H. J Am Chem Soc 2006, 128, 1995–2004.
17. Kritzer, J. A.; Lear, J. D.; Hodsdon, M. E.; Schepartz, A. J Am Chem Soc 2004, 126, 9468–9469.
18. Stephens, O. M.; Kim, S.; Welch, B. D.; Hodsdon, M. E.; Kay, M. S.; Schepartz, A. J Am Chem Soc 2005, 127, 13126–13127.
19. Seebach, D.; Hook, D. F.; Glattli, A. Biopolymers 2006, 84, 23–37.
20. Baldauf, C.; Gunther, R.; Hofmann, H. J. Phys Biol 2006, 3, S1–S9.
21. Baldauf, C.; Gunther, R.; Hofmann, H. J. J Org Chem 2006, 71, 1200–1208.
22. Baldauf, C.; Gunther, R.; Hofmann, H. J. Biopolymers 2006, 84, 408–413.
23. Orner, B. P.; Ernst, J. T.; Hamilton, A. D. J Am Chem Soc 2001, 123, 5382–5383.
24. Ernst, J. T.; Kutzki, O.; Debnath, A. K.; Jiang, S.; Lu, H.; Hamilton, A. D. Angew Chemie Int Ed 2002, 41, 278–281.
25. Kutzki, O.; Park, H. S.; Ernst, J. T.; Orner, B. P.; Yin, H.; Hamilton, A. D. J Am Chem Soc 2002, 124, 11838–11839.
26. Yin, H.; Lee, G. I.; Sedey, K. A.; Kutzki, O.; Park, H. S.; Omer, B. P.; Ernst, J. T.; Wang, H. G.; Sebti, S. M.; Hamilton, A. D. J Am Chem Soc 2005, 127, 10191–10196.
27. Yin, H.; Lee, G. I.; Park, H. S.; Payne, G. A.; Rodriguez, J. M.; Sebti, S. M.; Hamilton, A. D. Angew Chemie Int Ed 2005, 44, 2704–2707.
28. Bemis, G. W.; Murcko, M. A. J Med Chem 1996, 39, 2887–2893.
29. Yin, H.; Lee, G. I.; Sedey, K. A.; Rodriguez, J. M.; Wang, H. G.; Sebti, S. M.; Hamilton, A. D. J Am Chem Soc 2005, 127, 5463–5468.
30. Davis, J. M.; Truong, A.; Hamilton, A. D. Org Lett 2005, 7, 5405–5408.
31. Jacoby, E. Bioorg Med Chem Lett 2002, 12, 891–893.
32. Horwell, D. C.; Howson, W.; Ratcliffe, G. S.; Willems, H. M. G. Bioorg Med Chem 1996, 4, 33–42.
33. Kim, I. C.; Hamilton, A. D. Org Lett 2006, 8, 1751–1754.
34. Creamer, T. P.; Rose, G. D. Proteins 1994, 19, 85–97.
35. Creamer, T. P.; Rose, G. D. Proc Natl Acad Sci USA 1992, 89, 5937–5941.

Reviewing Editor: David Wemmer